imentally that both solvents used in the present study are not strongly perturbing solvents. Marcus[24] also has classified these as inert solvents. This classification is strongly supported by the experimental data on the total dipole moment of a toluene molecule having a similar electronic structure as benzene: 0.37 D in the gas phase and 0.43 D in inert solvents.[25] The ratio of the observed moments coincides with that calculated by eq 15. This means there exist no specific interactions between toluene (benzene) and inert solvents.

Thus, it can be concluded that the validity of our new equation is confirmed in dilute solution. Further work is of course necessary, and we are now attempting to test our equation in the liquid phase.

Acknowledgment. We express our deepest appreciation to Emeritus Professor Yuzo Kakiuti for making this study possible. Thanks are also due to Mr. Hiroshi Saito for his kind advice. We also thank Professor Gene S. Lehman for his kindness in reading the original manuscript.

Registry No. C_6H_6, 71-43-2.

(24) Marcus, Y. *Introduction to Liquid State Chemistry*; Wiley-Interscience: New York, 1977; Chapter 3.
(25) McClellan, A. L. *Tables of Experimental Dipole Moments*; W. H. Freeman and Company: San Francisco, 1963; p 251.

Crystal and Molecular Structure of the 2:1 Charge-Transfer Salt of Decamethylferrocene and Perfluoro-7,7,8,8-tetracyano-*p*-quinodimethane: $\{[Fe(C_5Me_5)_2]^{\cdot+}\}_2[TCNQF_4]^{2-}$. Electronic Structure of $[TCNQF_4]^n$ (n = 0, 1-, 2-)†

David A. Dixon,* Joseph C. Calabrese, and Joel S. Miller*

Central Research and Development Department, E. I. du Pont de Nemours & Co., Inc., Wilmington, Delaware 19898 *(Received: April 20, 1988; In Final Form: August 4, 1988)*

The reaction of decamethylferrocene, $Fe(C_5Me_5)_2$, and perfluoro-7,7,8,8-tetracyano-*p*-quinodimethane, $TCNQF_4$, leads to the isolation of two phases of 1:1 and 2:1 stoichiometry. The crystal and molecular structure of the black 2:1 substance has been determined by single-crystal X-ray analysis at -70 °C: $P\bar{1}$ space group (no. 2), a = 9.604 (1) Å, b = 9.789 (1) Å, c = 12.203 (1) Å, α = 91.33 (1)°, β = 92.05 (1)°, and γ = 93.61 (1)°, V = 1143.9 Å^3, and Z = 1. The cation is ordered and shows no unusual bond lengths or angles. The average Fe-C, C-C, and C-Me distances are 2.097, 1.428, and 1.495 Å, respectively. The dianion is nonplanar with the $-C(CN)_2$ groups forming a plane and the C_6 ring forming a second plane with a dihedral angle of 33.3°. The ring C-C distances range from 1.373 (3) to 1.401 (3) Å and are essentially equal to each other and the 1:389-Å distance accepted for an aromatic bond distance. The exocyclic C—$C(CN)_2$, C—CN, and C≡N average distances are 1.457, 1.403, and 1.155 Å, respectively. This structure is comprised of ···DADDAD··· chains (D = $[Fe(C_5Me_5)_2]^{\cdot+}$; A = $[TCNQF_4]^{2-}$). The DAD repeat unit possesses inversion symmetry. The $[TCNQF_4]^{2-}$ ion has been characterized by infrared, Raman, and UV-vis spectroscopic techniques, and the data are compared experimentally and theoretically to $[TCNQF_4]^{\cdot-}$ and $TCNQF_4$. Ab initio molecular orbital theory with the STO-3G basis set was used for the theoretical calculations. The geometries were gradient optimized for $[TCNQF_4]^n$ (n = 0, 1-, 2-). Force fields were calculated analytically for n = 0 and 2-. The 1:1 Fe (as well as the Co and Cr analogues) phases belong to the $P2_1/c$ monoclinic space group and are amorphous to the previously reported dimer phase of $[Fe(C_5Me_5)_2]_2[TCNQ]_2$ and contain the S = 0 $[TCNQF_4]_2^{2-}$ anion.

Introduction

The observation of metamagnetism[1] for the one-dimensional (1-D) phase of $[Fe(C_5Me_5)_2]^{\cdot+}[TCNQ]^{\cdot-}$ (TCNQ = 7,7,8,8-tetracyano-*p*-quinodimethane), as well as the observation of ferromagnetism for various phases of polycyanoanionic acceptors[2-4] and decamethylferrocene, has led us to undertake the systematic study of the structure-function relationship between planar strong acceptors and metallocenium donors. As a result of these studies we have discovered a series of D_2A (D = donor; A = acceptor) complexes enabling the structural and spectroscopic characterization of dianions,[5] e.g., $[TCNQF_4]^{2-}$, $[TCNE]^{2-}$,[6] $[TCNQ]^{2-}$,[7] $[C_6(CN)_6]^{2-}$,[8] $C_4(CN)_6]^{2-}$,[9] and $[DDQ]^{2-}$.[5] Herein we report the results of our structural, spectroscopic, and theoretical studies of $[TCNQF_4]^{2-}$ and compare these results with $[TCNQF_4]^{\cdot-}$[10] and $TCNQF_4$ as well as $[TCNQ]^n$ (n = 0, 1-, 2-).[7]

Experimental Section

Synthesis. $[Fe(C_5Me_5)_2]_2[TCNQF_4]$ was prepared from $Fe(C_5Me_5)_2$ (Organometallics, Inc., E. Hampsted, NH; Strem Chemical Co., Newburyport, NH) and $TCNQF_4$ in an inert atmosphere glovebox. Decamethylferrocene (150 mg; 0.46 mmol) dissolved in 30 mL of hot acetonitrile was added to a warm solution of 63 mg (0.23 mmol) $TCNQF_4$[11] dissolved in 3 mL of MeCN. Upon cooling to room temperature and vacuum filtration, 170 mg of the dark green-black crystalline product (80%) was col-

† Contribution No. 4720.

(1) Candela, G. A.; Swartzendruber, L. J.; Miller, J. S.; Rice, M. J. *J. Am. Chem. Soc.* **1979**, *101*, 2755.
(2) Miller, J. S.; Epstein, A. J.; Reiff, W. M. *Isr. J. Chem.* **1987**, *27*, 363. Miller, J. S.; Epstein, A. J.; Reiff, W. M. *Science* **1988**, *240*, 40-47. Miller, J. S.; Epstein, A. J.; Reiff, W. M. *Acc. Chem. Res.* **1988**, *21*, 114-120. Miller, J. S.; Epstein, A. J.; Reiff, W. M. *Chem. Rev.* **1988**, *88*, 201-200.
(3) (a) Miller, J. S.; Calabrese, J. C.; Epstein, A. J.; Bigelow, R. W.; Zhang, J. H.; Reiff, W. M. *J. Chem. Soc., Chem. Commun.* **1986**, 1026. (b) Miller, J. S.; Calabrese, J. C.; Chittapeddi, S.; Zhang, J. H.; Reiff, W. H.; Epstein, A. J. *J. Am. Chem. Soc.* **1987**, *109*, 769.
(4) Miller, J. S.; Zhang, J. H.; Reiff, W. M. *J. Am. Chem. Soc.* **1987**, *109*, 4584.
(5) Miller, J. S.; Dixon, D. A. *Science* **1987**, *235*, 871.
(6) Dixon, D. A.; Miller, J. S. *J. Am. Chem. Soc.* **1987**, *109*, 3656.
(7) Miller, J. S.; Zhang, J. H.; Reiff, W. M.; Dixon, D. A.; Preston, L. D.; Reis, A. H., Jr.; Gebert, E.; Extene, M.; Troup, J.; Epstein, A. J.; Ward, M. D. *J. Phys. Chem.* **1987**, *91*, 4344.
(8) Miller, J. S.; Ward, M. D.; Dixon, D. A.; Reiff, W. M.; Zhang, J. H. Manuscript in preparation.
(9) Miller, J. S.; Dixon, D. A.; Calabrese, J. C. Manuscript in preparation.
(10) Miller, J. S.; Zhang, J. H.; Reiff, W. M. *Inorg. Chem.* **1987**, *26*, 600.
(11) $TCNQF_4$ was prepared by: Wheland, R. C.; Martin, E. L. *J. Org. Chem.* **1975**, *40*, 3101.

0022-3654/89/2093-2284$01.50/0

TABLE I: Unit Cell Parameters for Dimeric 1:1 $M(C_5Me_5)_2TCNQ$ and $M(C_5Me_5)_2TCNQF_4$ Salts

	complex			
	$[Fe(C_5Me_5)_2]_2$-$[TCNQ]_2$[7]	$[Fe(C_5Me_5)_2]_2$-$[TCNQF_4]_2$	$[Co(C_5Me_5)_2]_2$-$[TCNQF_4]_2$	$[Cr(C_5Me_5)_2]_2$-$[TCNQF_4]_2$
a, Å	9.708	9.79	9.806	9.825
b, Å	12.211	12.35	12.310	12.458
c, Å	23.585	23.88	23.879	23.963
β, deg	95.012	94.52	94.01	94.81
V, Å^3	2785.1	2882.0	2875.4	2922.7
space group	$P2_1/c$	$P2_1/c$	$P2_1/c$	$P2_1/c$

lected. Anal. (Galbraith, Knoxville, TN) Calcd for $C_{26}H_{30}FeF_2N_2$: C, 67.25; H, 6.51; Fe, 12.03; F, 8.18; N, 6.03. Found: C, 67.19; H, 6.71; N, 6.71. Infrared spectra (Nujol), ν(C≡N) 2167 (s) and 2133 (s) cm^{-1}.

$[Co(C_5Me_5)_2]_2[TCNQF_4]$ was prepared analogously to the above reaction except that decamethylcobaltocene was prepared from $[Co(C_5Me_5)_2]^+[PF_6]^-$ (Strem) by a literature route (71%).[12] Anal. Calcd for $C_{26}H_{30}CoF_2N_2$: C, 66.80; H, 6.47; N, 5.99. Found: C, 66.80; H, 6.67; N, 6.11. Infrared spectra (Nujol), ν(C≡N) 2168 (s) and 2133 (s) cm^{-1}.

$[Fe(C_5Me_5)_2]_2[TCNQF_4]_2$ was prepared in a similar fashion to the above reaction except equal moles of $Fe(C_5Me_5)_2$ (e.g., 150 mg; 0.460 mmol, 15 mL of hot MeCN) per equivalent of $TCNQF_4$ (e.g., 127 mg; 0.460 mmol, 10 mL of warm MeCN) were utilized. After boiling off the solvent from the resultant dark green solution and cooling at room temperature overnight, black crystals formed that were ultimately collected via vacuum filtration (224 mg, 81%). Unit cell data on the single crystal was obtained as a means for characterizing the compound (Table I). Anal. Calcd for $C_{32}H_{30}FeF_4N_4$: C, 63.80; H, 5.02; N, 9.30; Fe, 9.27; F, 12.61. Found: C, 64.22; H, 5.02; N, 9.39; F, 12.61. Infrared spectra (Nujol), ν(C≡N) 2178 (s), 2195 (s), and 2198 (s) cm^{-1}.

$[Co(C_5Me_5)_2]_2[TCNQF_4]_2$ was prepared in a similar fashion to the above reaction except equal moles of $Co(C_5Me_5)_2$ (e.g., 100 mg; 0.304 mmol, 7 mL of hot MeCN) per equivalent of $TCNQF_4$ (e.g., 84 mg; 0.304 mmol, 1 mL of warm MeCN) were utilized. After boiling off the solvent from the resultant dark green solution and cooling at −25 °C overnight, black crystals formed that were ultimately collected via vacuum filtration (155 mg, 84%). Unit cell data on the single crystal are given in Table I. Anal. Calcd for $C_{32}H_{30}CoF_4N_4$: C, 63.47; H, 5.00; N, 9.25. Found: C, 63.62; H, 4.90; N, 9.28. Infrared spectra (Nujol), ν(C≡N) 2179 (s) and 2196 (s) cm^{-1}.

$[Cr(C_5Me_5)_2]_2[TCNQF_4]_2$ was prepared in a similar fashion to the above reaction except equal moles of $Cr(C_5Me_5)_2$[12] (e.g., 100 mg; 0.304 mmol, 7 mL of hot MeCN) per equivalent of $TCNQF_4$ (e.g., 84 mg; 0.304 mmol, 1 mL of warm MeCN) were utilized. After boiling off the solvent from the resultant dark green solution and cooling at −25 °C overnight, black crystals formed that were ultimately collected via vacuum filtration (155 mg, 84%). Unit cell data on the single crystal are given in Table I. Anal. Calcd for $C_{32}H_{30}CrF_4N_4$: C, 64.20; H, 5.05; N, 9.36; F, 12.70. Found: C, 62.68; H, 5.17; N, 9.28. Infrared spectra (Nujol), ν(C≡N) 2179 (s) and 2196 (s) cm^{-1}.

Collection and Reduction of X-ray Data for $[Fe(C_5Me_5)_2]_2[TCNQF_4]$. The crystal structure data were obtained from a dark green parallelpiped crystal (0.48 × 0.42 × 0.53 mm) on a CAD4 diffractometer equipped with a Mo Kα source, graphite monochromator, and a FTS LT1 low-temperature device operating at −70 °C. Preliminary diffractometer results indicated a triclinic unit cell with space group $P\bar{1}$ (no. 2) based on 23 reflections. A summary of the data acquisition and unit cell data is given in Table II. A total of 5442 data were collected with ω-scans from 3.3° < 2θ < 55° yielding 3634 unique reflections with $I > 3\sigma(I)$ for the analysis. The intensities of the standard reflections (which were collected 39 times) were adjusted for a 34% isotropic decrease in intensity. The data were reduced in the usual fashion, excluding absorption effects due to the small absorption coefficient and the nearly isotropic shape of the crystal. The intensities were phased via automatic Patterson analysis which revealed the cation in a general position with the anion on an inversion center.[13] Scattering factors were obtained from standard tables and included anomalous terms for Fe.[14] A total of 400 parameters were refined with all non-hydrogen atoms refined anisotropically and all hydrogen atoms refined isotropically. The final value for R is 0.033 with R_w = 0.039 with an error of fit of 1.62. The largest peak on the final difference Fourier is 0.25 e$^-$/Å^3 bisecting C1 and C2.

TABLE II: Crystallographic Details for $\{[Fe^{III}C_5Me_5)_2]^{\bullet+}\}_2[TCNQF_4]^{2-}$

formula	$C_{26}H_{30}FeF_2N_2$
formula mass	464.4
space group	$P\bar{1}$ (no. 2)
a, Å	9.604 (1)
b, Å	9.789 (1)
c, Å	12.203 (1)
α, deg	91.33 (1)
β, deg	92.05 (1)
γ, deg	93.61 (1)
V, Å^3	1143.9
Z	2
ρ(calcd), g cm^{-3}	1.348
cryst dimensions, mm	0.48 × 0.42 × 0.53
μ (Mo Kα), cm^{-1}	6.88
temperature, °C	−70
radiation	Mo Kα
scan mode	ω
2θ max, deg	55.0
total data measured	5442
unique data with $(F_o)^2 > 3\sigma(F_o)^2$	3634
final number variables	400
weighting scheme	$\propto[\sigma^2 + 0.009I^2]^{-1/2}$
R_u[a]	0.033
R_w[b]	0.039
largest residual, e$^-$ Å^{-3}	0.25
diffractometer	Enraf-Nonius CAD4

[a] $R_u = \sum(|F_o| - |F_c|)^2/\sum(|F_o|)^2$. [b] $R_w = \sum w(|F_o| - |F_c|)^2/\sum w(|F_o|)^2$.

Spectroscopic Measurements. The infrared spectra were recorded on a Nicolet 7199 Fourier transform spectrometer. The UV–visible spectra were recorded on a Cary 2390 spectrometer.

Molecular Orbital Calculations. The geometries for $[TCNQF_4]^n$ (n = 0, 1−, 2−) were gradient optimized[15] at the SCF level in D_{2h} symmetry. The STO-3G basis set[16] (100 basis functions) was used for all calculations. For the closed-shell species with n = 0 and n = 2−, the geometries were optimized in the RHF framework with the program GRADSCF[17] on a CRAY-1A com-

(12) Robbins, J. L.; Edelstein, M.; Spenser, B.; Smart, J. C. *J. Am. Chem. Soc.* **1982**, *104*, 1882.

(13) A second determination yielded a = 9.583 (5) Å, b = 9.807 (5) Å, c = 12.200 (6) Å, α = 91.35 (3)°, β = 92.06 (3)°, γ = 93.69 (3)°, T = −70 °C, V = 1143 Å^3, R_u = 0.070, and R_w = 0.084.

(14) (a) Cromer, D. T.; Waber, J. T. *International Tables for X-Ray Crystallography*; Kynoch Press: Birmingham, England, 1974; Vol. IV, Table 2.2B. (b) Cromer, D. T.; Waber, J. T. *International Tables for X-Ray Crystallography*; Kynoch Press: Birmingham, England, 1974; Vol. IV, Table 2.3.1.

(15) (a) Komornicki, A.; Ishida, K.; Morokuma, K.; Ditchfield, R.; Conrad, M. *Chem. Phys. Lett.* **1977**, *45*, 595. McIver, J. W., Jr.; Komornicki, A. *Chem. Phys. Lett.* **1971**, *10*, 303. (b) Pulay, P. In *Applications of Electronic Structure Theory*; Schaefer, H. F., III, Ed.; Plenum: New York, 1977; p 153.

(16) Hehre, W. J.; Stewart, R. F.; Pople, J. A. *J. Chem. Phys.* **1969**, *51*, 2657.

TABLE III: Fractional Coordinates (×10⁴) and Isotropic Thermal Parameters for $[Fe(C_5Me_5)_2]_2[TCNQF_4]$

atom	x	y	z	B_{iso}[a]
Fe(1)	1985.8 (3)	1840.7 (3)	2169.6 (3)	1.6 (1)′
F(2)	4150 (1)	7430 (1)	4312 (1)	2.7 (1)′
F(3)	2897 (1)	6251 (1)	5953 (1)	2.7 (1)′
N(5)	5142 (2)	7670 (2)	1724 (2)	3.6 (1)′
N(6)	9002 (2)	6145 (2)	2875 (2)	3.8 (1)′
C(1)	5698 (2)	5659 (2)	4089 (2)	1.9 (1)′
C(2)	4589 (2)	6201 (2)	4623 (2)	1.9 (1)′
C(3)	3929 (2)	5584 (2)	5478 (2)	1.9 (1)′
C(4)	6400 (2)	6319 (2)	3183 (2)	2.0 (1)′
C(5)	5692 (2)	7068 (2)	2399 (2)	2.3 (1)′
C(6)	7827 (2)	6202 (2)	3019 (2)	2.4 (1)′
C(10)	3914 (2)	1881 (2)	3048 (2)	2.3 (1)′
C(11)	3875 (2)	3041 (2)	2360 (2)	2.2 (1)′
C(12)	2733 (2)	3815 (2)	2686 (2)	2.1 (1)′
C(13)	2072 (2)	3131 (2)	3563 (2)	2.2 (1)′
C(14)	2805 (2)	1931 (2)	3789 (2)	2.4 (1)′
C(15)	4982 (3)	833 (3)	3025 (3)	3.7 (1)′
C(16)	4880 (3)	3410 (3)	1494 (3)	3.3 (1)′
C(17)	2329 (3)	5136 (3)	2220 (3)	3.0 (1)′
C(18)	855 (3)	3615 (3)	4164 (3)	3.2 (1)′
C(19)	2490 (4)	947 (3)	4674 (3)	3.8 (1)′
C(20)	99 (2)	629 (2)	1957 (2)	2.2 (1)′
C(21)	1245 (2)	−126 (2)	1622 (2)	2.1 (1)′
C(22)	1900 (2)	591 (2)	754 (2)	2.0 (1)′
C(23)	1172 (2)	1792 (2)	556 (2)	2.1 (1)′
C(24)	56 (2)	1815 (2)	1304 (2)	2.2 (1)′
C(25)	−898 (3)	220 (4)	2823 (3)	3.6 (1)′
C(26)	1675 (3)	−1443 (3)	2079 (3)	3.2 (1)′
C(27)	3125 (3)	138 (3)	140 (2)	2.8 (1)′
C(28)	1495 (3)	2817 (3)	−301 (2)	3.3 (1)′
C(29)	−993 (3)	2888 (3)	1359 (3)	3.3 (1)′
H(15)	5709 (38)	1106 (36)	3488 (31)	6.6 (9)
H(15′)	5389 (37)	766 (36)	2241 (32)	7.0 (10)
H(15″)	4629 (35)	−118 (38)	3212 (30)	6.9 (9)
H(16)	5706 (32)	3886 (30)	1825 (25)	4.9 (7)
H(16′)	4463 (38)	4055 (37)	921 (31)	7.5 (10)
H(16″)	5170 (35)	2677 (37)	1117 (30)	6.3 (9)
H(17)	2574 (34)	5222 (33)	1482 (29)	5.6 (8)
H(17′)	2805 36)	5821 (37)	2628 (29)	6.6 (9)
H(17″)	1355 (32)	5178 (28)	2213 (24)	4.5 (7)
H(18)	1177 (33)	4130 (34)	4773 (29)	5.9 (9)
H(18′)	301 (36)	2963 (35)	4372 (29)	5.7 (9)
H(18″)	207 (36)	4101 (35)	3678 (29)	6.5 (9)
H(19)	1472 (39)	836 (36)	4822 (29)	7.3 (10)
H(19′)	2969 (33)	1228 (32)	5330 (28)	5.5 (8)
H(19″)	2792 (36)	33 (39)	4513 (29)	7.0 (10)
H(25)	−1740 (36)	−287 (34)	2531 (29)	6.6 (9)
H(25′)	−1210 (36)	952 (38)	3249 (29)	6.7 (10)
H(25″)	−514 (38)	−417 (39)	3366 (32)	7.9 (11)
H(26)	2615 (37)	−1488 (33)	2103 (28)	6.0 (8)
H(26′)	1330 (40)	−2167 (41)	1613 (35)	8.4 (11)
H(26″)	1305 (42)	−1691 (41)	2716 (37)	8.6 (12)
H(27)	3720 (28)	944 (29)	−94 (22)	4.0 (6)
H(27′)	2818 (30)	−295 (30)	−520 (26)	4.7 (7)
H(27″)	3735 (35)	−464 (35)	575 (28)	6.5 (9)
H(28)	2518 (37)	2969 (33)	−395 (27)	6.4 (9)
H(28′)	1193 (36)	3627 (38)	−104 (29)	6.7 (10)
H(28″)	1036 (33)	2531 (32)	−997 (29)	5.6 (8)
H(29)	−1487 (36)	2913 (34)	2059 (32)	6.5 (9)
H(29′)	−1661 (37)	2766 (36)	796 (32)	7.1 (10)
H(29″)	−556 (38)	3840 (39)	1220 (30)	7.2 (9)

[a] $B_{iso} = {}^4/_3\sum_{i=1}^{3}\sum_{j=1}^{3}(a_i \cdot a_j)B_{ij}$.

puter. The force fields for the closed-shell species were obtained analytically[18] with the program GRADSCF. The calculations on the open-shell-doublet anion were done in the UHF framework with the program HONDO[19] on an IBM 3081 computer.

(17) GRADSCF is an ab initio gradient program system designed and written by A. Komornicki at Polyatomics Research.

(18) King, H. F.; Komornicki, A. In *Geometrical Derivatives of Energy Surfaces and Molecular Properties*; Jorgenson, P.; Simon, S., Eds.; NATO ASI Series C 166; Reidel: Dordrecht, 1986; p 207. King, H. F.; Komornicki, A. *J. Chem. Phys.* **1986**, *84*, 5645.

TABLE IV: Anisotropic Thermal Parameters for $[Fe(C_5Me_5)_2]_2[TCNQF_4]$ (10^4 Å)[a]

atom	U_{11}	U_{22}	U_{33}	U_{12}	U_{13}	U_{23}
Fe(1)	19.3 (1)	20.0 (2)	21.2 (2)	2.5 (1)	0.9 (1)	2.8 (1)
F(2)	41.8 (7)	24.6 (7)	40.3 (8)	12.0 (5)	11.7 (6)	11.8 (6)
F(3)	34.9 (7)	30.7 (7)	40.2 (9)	11.6 (5)	16.3 (6)	7.5 (6)
N(5)	39 (1)	56 (1)	47 (1)	15 (1)	14 (1)	25 (1)
N(6)	34 (1)	64 (2)	51 (2)	12 (1)	12 (1)	32 (1)
C(1)	24 (1)	24 (1)	23 (1)	−1 (1)	3 (1)	3 (1)
C(2)	27 (1)	18 (1)	28 (1)	4 (1)	1 (1)	5 (1)
C(3)	22 (1)	24 (1)	28 (1)	4 (1)	5 (1)	0 (1)
C(4)	26 (1)	25 (1)	26 (1)	2 (1)	5 (1)	5 (1)
C(5)	25 (1)	28 (1)	37 (1)	2 (1)	10 (1)	9 (1)
C(6)	31 (1)	33 (1)	27 (1)	3 (1)	6 (1)	11 (1)
C(10)	25 (1)	29 (1)	34 (1)	6 (1)	−8 (1)	−4 (1)
C(11)	22 (1)	28 (1)	34 (1)	−2 (1)	0 (1)	−4 (1)
C(12)	25 (1)	24 (1)	29 (1)	1 (1)	−2 (1)	−1 (1)
C(13)	29 (1)	31 (1)	25 (1)	7 (1)	−2 (1)	−1 (1)
C(14)	35 (1)	31 (1)	24 (1)	4 (1)	−7 (1)	2 (1)
C(15)	35 (1)	41 (2)	65 (2)	17 (1)	−14 (2)	−9 (2)
C(16)	29 (1)	47 (2)	49 (2)	−6 (1)	12 (1)	−4 (1)
C(17)	38 (1)	23 (1)	52 (2)	3 (1)	−4 (1)	5 (1)
C(18)	38 (1)	52 (2)	32 (2)	10 (1)	8 (1)	−6 (1)
C(19)	68 (2)	48 (2)	30 (2)	4 (2)	−6 (2)	15 (1)
C(20)	22 (1)	32 (1)	28 (1)	−1 (1)	3 (1)	3 (1)
C(21)	24 (1)	22 (1)	32 (1)	−1 (1)	−3 (1)	2 (1)
C(22)	23 (1)	27 (1)	24 (1)	−1 (1)	0 (1)	−1 (1)
C(23)	28 (1)	29 (1)	23 (1)	1 (1)	−2 (1)	3 (1)
C(24)	23 (1)	28 (1)	30 (1)	2 (1)	−3 (1)	0 (1)
C(25)	30 (1)	58 (2)	47 (2)	−5 (1)	14 (1)	8 (2)
C(26)	35 (1)	25 (1)	63 (2)	2 (1)	0 (1)	13 (1)
C(27)	34 (1)	40 (1)	33 (2)	2 (1)	10 (1)	−7 (1)
C(28)	50 (2)	47 (2)	30 (1)	0 (1)	−3 (1)	17 (1)
C(29)	33 (1)	40 (2)	52 (2)	14 (1)	−7 (1)	−2 (1)

[a] $\exp[-2\pi^2(U_{11}h^2a^{*2}... + 2(U_{12}hka^*b^*...))]$.

TABLE V: Interatomic Anion Bond Distances and Angles for $[Fe(C_5Me_5)_2]_2[TCNQF_4]$

	Bond Distances, Å		
F(2)–C(2)	1.358 (2)	C(1)–C(3)[a]	1.401 (3)
F(3)–C(3)	1.360 (2)	C(1)–C(4)	1.457 (3)
N(5)–C(5)	1.156 (3)	C(2)–C(3)	1.373 (3)
N(6)–C(6)	1.153 (3)	C(4)–C(5)	1.402 (3)
C(1)–C(2)	1.394 (3)	C(4)–C(6)	1.404 (3)
	Intramolecular Angles, deg		
F(2)–C(2)–C(1)	118.9 (2)	C(2)–C(1)–C(3)[a]	112.7 (2)
F(2)–C(2)–C(3)	117.2 (2)	C(2)–C(1)–C(4)	123.8 (2)
F(3)–C(3)–C(1)[a]	118.7 (2)	C(3)[a]–C(1)–C(4)	123.6 (2)
F(3)–C(3)–C(2)	117.8 (2)	C(1)–C(2)–C(3)	123.9 (2)
N(5)–C(5)–C(4)	177.5 (3)	C(1)[a]–C(3)–C(2)	123.4 (2)
N(6)–C(6)–C(4)	178.1 (3)	C(1)–C(4)–C(5)	122.5 (2)
		C(1)–C(4)–C(6)	121.9 (2)
		C(5)–C(4)–C(6)	115.5 (2)

[a] Symmetry operation codes: $1 - x, 1 - y, 1 - z$.

Results and Discussion

Crystal Data Analysis. 1:1 Salts. The $TCNQF_4$ 1:1 salts with $M(C_5Me_5)_2$ (M = Fe, Cr, Co) are isostructural to each other and $[Fe(C_5Me_5)_2]_2[TCNQ]_2$.[7] Each complex belongs to the $P2_1/c$ monoclinic space group, and the lattice parameters are summarized in Table I. Consequently their structure consists of a herringbone array of DAAD dimers (D = metallocene cation donor; A = TCNQ anion acceptor). Attempts to prepare a linear chain phase as present for metamagnetic $[Fe(C_5Me_5)_2]^{\bullet+}[TCNQ]^{\bullet-}$[1,7] were unsuccessful. Rapid precipitation, which is necessary to form the kinetic $[Fe(C_5Me_5)_2]^{\bullet+}[TCNQ]^{\bullet-}$[1,7] phase, led only to isolation of the dimer phase.

2:1 Salts. $[Fe(C_5Me_5)_2]_2[TCNQF_4]$. The triclinic unit cell is comprised of an independent ordered cation with approximate D_{5d} symmetry and half of an independent anion. Fractional

(19) (a) Dupuis, M.; Rys, J.; King, H. F. *J. Chem. Phys.* **1976**, *65*, 111. (b) King, H. F.; Dupuis, M.; Rys, J. *National Resource for Computer Chemistry Software Catalog, Vol 1*; Program QHO2 (HONDO), 1980.

TABLE VI: Observed and Calculated Structural Parameters for $[TCNQF_4]^n$ (n = 0, 1-, 2-)[a,b]

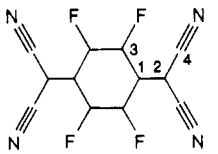

parameter	n = 0	n = 0	n = 0	n = 1-	n = 1-	n = 1-	n = 1-	n = 1-	n = 2-	n = 2-
$r(C_3-C_3)$	1.334	1.331	1.343	1.353	1.350	1.360	1.345	1.368	1.373	1.397
$r(C_1-C_3)$	1.437	1.439	1.486	1.415	1.410	1.420	1.418	1.437	1.398	1.408
$r(C_1-C_2)$	1.372	1.373	1.350	1.415	1.413	1.429	1.418	1.421	1.457	1.466
$r(C_2-C_4)$	1.437	1.438	1.460	1.429	1.417	1.435	1.423	1.437	1.403	1.417
$r(C_4-N)$	1.140	1.149	1.158	1.144	1.144	1.140	1.148	1.188	1.154	1.164
$r(C_3-F)$	1.336	1.334	1.352	1.354	1.346	1.349	1.359	1.364	1.359	1.366
$\theta(C_1C_3C_3)$	123.2	122.8	122.5	123.7	123.6	124	123.9	122.7	123.6	123.5
$\theta(C_3C_1C_3)$	113.5	114.5	115.0	112.5	112.7	111	112.2	114.7	112.7	113.1
$\theta(C_2C_1C_3)$	123.2	127.7	122.5	123.8	123.5	124	123.7	122.7	123.7	123.5
$\theta(C_1C_2C_4)$	123.8	123.7	123.2	124.1	123.5	124	123.8	122.5	122.2	122.2
$\theta(C_4C_2C_4)$	112.6	112.5	113.6	111.9	113.2	113	112.2	115.0	115.5	115.7
$\theta(C_1C_4N)$	175.2	174.4	177.8	174.0	176.3	174	174.9	177.4	177.8	177.1
$\theta(C_1C_3F)$	118.1	118.4	117.6	118.5	118.6	118	118.0	118.9	118.8	119.8
$\theta(C_3C_3F)$	118.7	118.8	119.9	117.8	117.8	119	118.0	118.5	117.5	116.7
T, °C	RT	-97		RT	RT	RT	-97		-100	
R	3.6	6.8		7.2	6.9	6.8	6.8		3.3	
dimer, Å		3.155			3.150	3.225	3.155			
source	$TCNQF_4$	$[Fe(C_5H_5)_2]_2$-$[TCNQF_4]_3$	STO-3G RHF	[Me_2Phen]-$[TCNQF_4]$	[N-BuPhen]-$[TCNQF_4]$	$[Fe(C_5H_5)_2]$-$[TCNQF_4]$	$[Fe(C_5H_5)_2]_2$-$[TCNQF_4]_3$	STO-3G UHF	$[Fe(C_5H_5)_2]_2$-$[TCNQF_4]$	STO-3G RHF
ref	20	10[c]		21	22	10	10[c]			

[a] Bond distances in Å. Bond angles in deg. [b] Averaged over chemically equivalent distances and angles. [c] In a dimer structure.

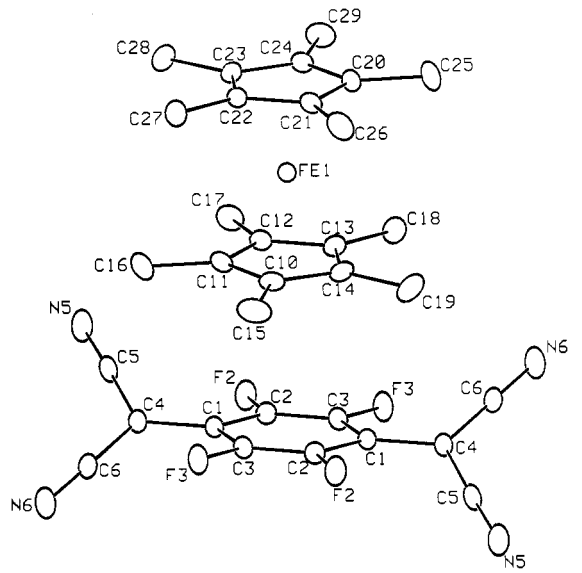

Figure 1. Atom labeling for the crystal structure (25% ellipsoids) of $[Fe(C_5Me_5)_2]_2[TCNQF_4]$.

coordinates, anisotropic thermal parameters and general temperature factors, and anion interatomic bond distances and angles are in Tables III, IV, and V, respectively. Atom labeling for the independent cation and anion is shown in Figure 1. The cation bond distances and angles, intermolecular and intramolecular distances, and deviations from the weighted least-squares planes are given as supplementary material (see paragraph regarding supplementary material at the end of the paper).

$[Fe(C_5Me_5)_2]^{+}$. The cation is ordered with approximate molecular D_{5d} symmetry and possesses distances essentially equivalent to previously characterized $[Fe(C_5Me_5)_2]^{+}$ cations.[3b] The Fe–C, C–C, and C–Me distances range between 2.090 (2) and 2.107 (2) Å (average = 2.097 Å), between 1.424 (3) and 1.434 (3) Å (average = 1.428 Å), and between 1.490 (3) and 1.503 (3) Å (average = 1.495 Å), respectively. The Fe–C_5 ring centroid ranges from 1.708 to 1.717 Å with an average of 1.713 Å.

$[TCNQF_4]^{2-}$. The structure of the dianion has been determined for the first time and is of interest particularly for comparison with the structures of $[TCNQF_4]^n$ (n = 0, 1-) and $[TCNQ]^n$ (n = 0, 1-, 2-). The details of the structure for $[TCNQF_4]^{2-}$ are summarized in Table VI and Figure 2 together with the $[TCNQF_4]^n$ (n = 0, 1-) structural data.[10,20-22] The most striking

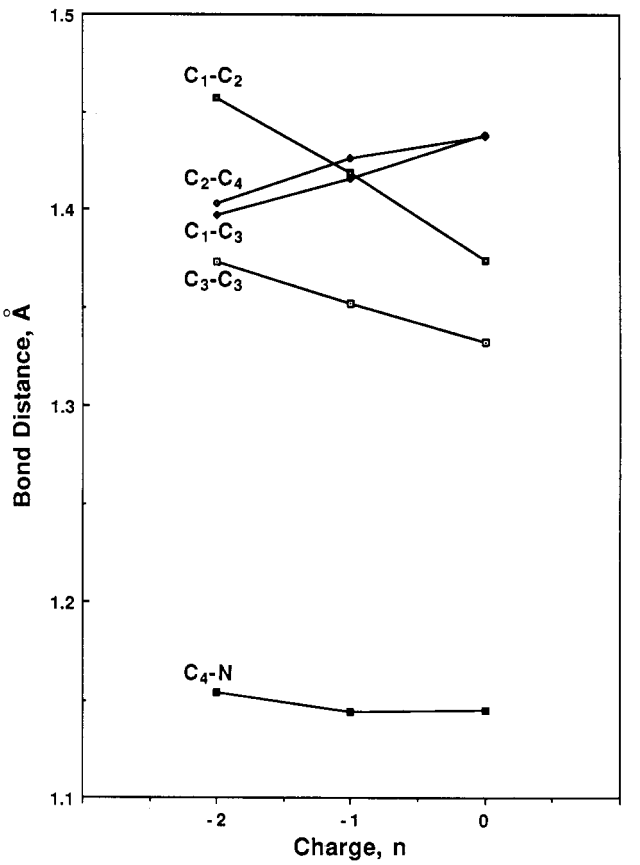

Figure 2. Bond distance as a function of n for $[TCNQF_4]^n$ (n = 0, 1-, 2-). Labeling is as shown in Table V.

(20) Emge, T. J.; Maxfield, M.; Cowan, D. O.; Kistenmacher, T. *J. Mol. Cryst. Liq. Cryst.* **1981**, *65*, 161–178.
(21) Soos, Z. G.; Keller, H. J.; Ludolf, K.; Queckborner, J.; Wehe, D.; Flandrois, S. *J. Chem. Phys.* **1981**, *76*, 5287–5294.

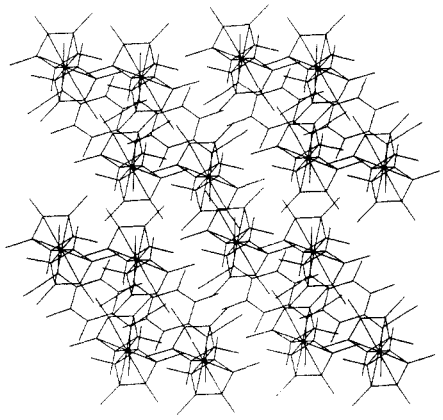

Figure 3. Stereoview of the unit cell of $[Fe(C_5Me_5)_2]_2[TCNQF_4]$.

feature is that the $TCNQF_4$ dianion, unlike $[TCNQF_4]^n$ (n = 0, 1-) and $[TCNQ]^n$ (n = 0, 1-, 2-)[7] which have planar D_{2h} symmetry, is nonplanar. The C_6 ring and $C(CN)_2$ groups are planar (Table VI), and the $[C(CN)_2]^-$ groups are both in a plane canted 33.3° from the plane of the C_6 ring (Figure 1); i.e., the rotation about the C_1–C_4 nominal single bonds is in the same sense. The central bond in the ring, C_3–C_3, is 1.373 (3) Å, which is 0.043 and ~0.03 Å longer than the bond for $[TCNQF_4]^n$, n = 1- and 0, respectively. The other C–C ring bonds are slightly longer and more benzene-like, averaging 1.398 Å. The C_2–C_4 bonds are of comparable length, 1.403 Å. Only the C_1–C_2 bonds are long, 1.457 Å. The C≡N bond lengths average 1.154 Å and are slightly longer than those in the n = 0 or n = 1- ions.

The bond distances as a function of n for $[TCNQF_4]^n$ are summarized in Figure 2. On the basis of the previous results found in $[TCNQ]^n$ (n = 0, 1-, 2-), experimentally and from numerous theoretical studies,[7] we would expect to see a lengthening in the C_1–C_2 bond as charge is added so that this bond closely resembles a C–C single bond in the dianion. As a consequence, the ring should become more benzenoid with all of the ring C–C bond lengths approaching the same value as is observed. The C–F bonds should lengthen while the C_2–C_4 bonds shorten as the added negative charge is distributed over as many centers as possible. The C≡N bond length increases slightly as the more negative charge, but this result is only qualitative due to the error limits in the various structure determinations. The angles show only small changes as negative charge is added. The angle $\theta(C_4C_2C_4)$ increases as the negative charge is increased, and the C≡N bonds apparently become more linear. The increase in $\theta(C_4C_2C_4)$ is consistent with the shortening of the C_2–C_4 bond.

Solid-State Structure. The solid is comprised of segregated columns of cations and anions in a ···DADDAD··· array which is best seen in the stereoview, Figure 3. There are three unique pairwise chain interactions, i.e., I–II, I–III, and I–IV (Figure 4). The intrachain Fe–Fe separations are 9.171 and 10.487 Å whereas intrachain Fe–Fe separations range from 8.750 to 12.200 Å (Figure 5).

UV–Visible Spectrum. The UV–visible spectra of $TCNQF_4$, $[Co(C_5Me_5)_2][TCNQF_4]$, and $[Co(C_5Me_5)_2]_2[TCNQF_4]$ are shown in Figure 6. The spectrum of $TCNQF_4$ has two peaks in the visible, near 25 000 cm^{-1}. The spectrum for $[TCNQF_4]^{\bullet-}$ has a low energy band near 12 000 cm^{-1} and a visible transition near 23 000 cm^{-1} that is red-shifted from the $TCNQF_4$ transition. These two features in $[TCNQF_4]^{\bullet-}$ are in agreement with previous observations.[23] The peak in $[Co(C_5Me_5)_5][TCNQF_4]$ near 35 000 cm^{-1} is due to transitions in the cation. The spectrum of $[Co(C_5Me_5)_2]_2[TCNQF_4]$ has two peaks considerably blue shifted from the $TCNQF_4$ visible transition. The higher energy peak is clearly due to the cation and has approximately twice the intensity of the cation peak in $[Co(C_5Me_5)_2][TCNQF_4]$ as would be expected. The other transition at ~30 000 cm^{-1} is due to the dianion

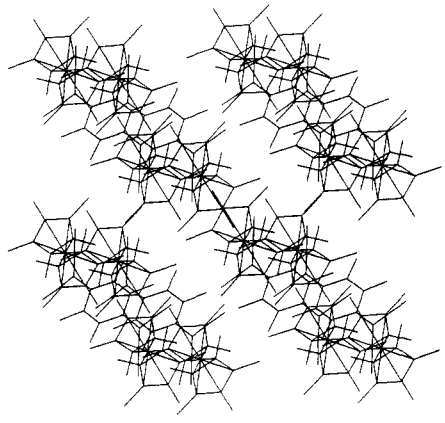

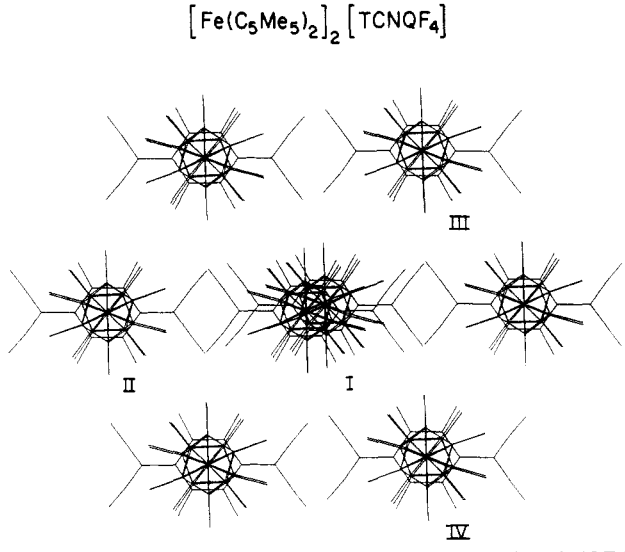

Figure 4. View normal to the 1-D chains of $[Fe(C_5Me_5)_2]_2[TCNQF_4]$ showing the unique chains, I–IV.

$[TCNQF_4]^{2-}$. The considerable blue shift compared to $TCNQF_4$ is consistent with the two additional electrons in $[TCNQF_4]^{2-}$ filling the low-lying LUMO of $TCNQF_4$. The LUMO of $TCNQF_4$ becomes the HOMO in $[TCNQF_4]^{2-}$, and there is now no very low-lying LUMO leading to a higher energy transition.

Molecular Orbital Calculation Structure. The calculated structural parameters for $[TCNQF_4]^n$ (n = 0, 1-, 2-) are given in Table VI. The calculated structure for $TCNQF_4$ is in good agreement with the experimental ones considering the small basis set. The single bonds in the ring, C_1–C_3, are calculated to be too long by 0.05 Å, and the double bonds in the ring are calculated to be too long by only 0.01 Å. The exocyclic double bond C_1–C_2 is too short by 0.02 Å. The C_2–C_4 single bonds are again calculated to be too long by 0.02 Å whereas the C≡N bond is calculated to be 0.01–0.02 Å too long. However, the calculated value for r(C≡N) is essentially the same as the value of 1.157 Å determined by microwave spectroscopy for CH_3CN.[24] The above calculated results are essentially the same as those calculated for TCNQ.[7] The C–F bonds are calculated to be 0.015–0.020 Å too long which is expected with this size basis set. The agreement between the calculated and experimental bond angles for $TCNQF_4$ is excellent. Theory predicts $\theta(C_2C_4N)$ to show less deviation from linearity than found experimentally. Both $\theta(C_3C_1C_3)$ and $\theta(C_4C_2C_4)$ are calculated to be 1° larger than the experimental values. Comparison of the calculated angles for $TCNQF_4$ with those for TCNQ shows some differences. The value of $\theta(C_3C_1C_3)$ in $TCNQF_4$ is calculated to be 1.5° smaller than the value in TCNQ, and an even larger difference is found for $\theta(C_4C_2C_4)$ with the angle in $TCNQF_4$ being 2.8° smaller. The

(22) Metzger, R. M.; Heimer, N. E.; Gundel, D.; Sixl, H.; Harms, R. H.; Keller, H. J.; Nothe, D.; Wehe, D. *J. Chem. Phys.* **1982**, *77*, 6203–6214.
(23) Zanon, I.; Pecile, C. *J. Phys. Chem.* **1983**, *87*, 3657.
(24) Costain, C. C. S. *J. Chem. Phys.* **1958**, *29*, 864.

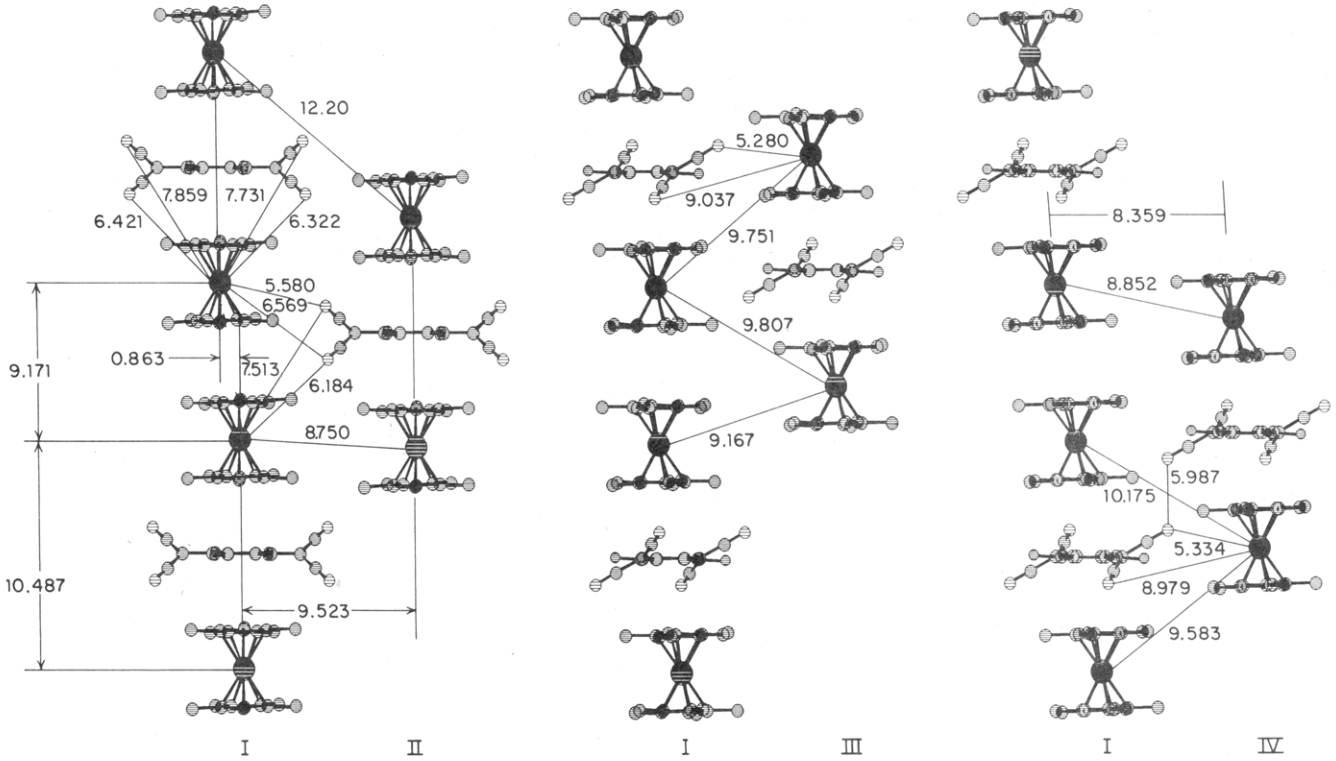

Figure 5. Out-of-registry interactions between chains I–II (left), I–III (middle), and I–IV (right).

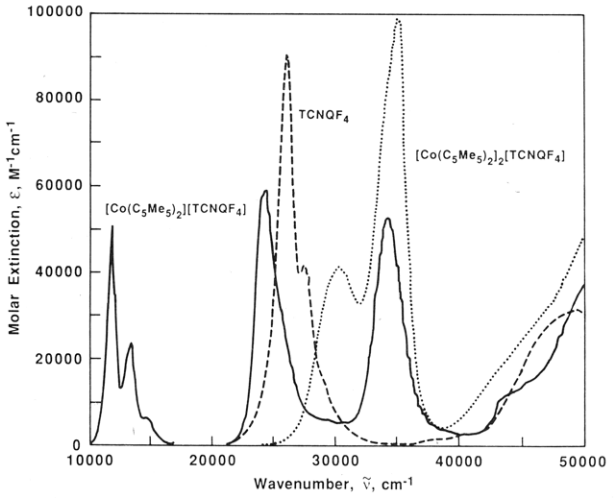

Figure 6. Electronic absorption spectra for $[TCNQF_4]^n$ (n = 0, 1–, 2–).

C_2C_4N bond angle is predicted to deviate from linearity by 1.1° in TCNQ as compared to 2.2° in $TCNQF_4$.

The calculated structure for $[TCNQF_4]^{\bullet-}$ shows even better agreement with the experimental values with the bond distances within 0.02 Å of the experimental values except for r(C≡N). As previously observed in $[TCNQ]^{\bullet-}$, the UHF formalism seems to make the C≡N bond too long when compared to experiment. The calculations predict a lengthening of the C–F bond in $[TCNQF_4]^{\bullet-}$ as is found experimentally. The value of $\theta(C_3C_1C_3)$ is predicted to decrease but by less than what is found experimentally. The angle $\theta(C_4C_2C_4)$ is predicted to increase in $[TCNQF_4]^{\bullet-}$ as compared to $TCNQF_4$, but the experimental scatter is too large to show this prediction. The major difference in the calculated structures of $[TCNQ]^{\bullet-}$ and $[TCNQF_4]^{\bullet-}$ is in $r(C_3–C_3)$, which is 0.013 Å longer in $[TCNQF_4]^{\bullet-}$. The bond angles in $[TCNQF_4]^{\bullet-}$ and $[TCNQ]^{\bullet-}$ are all quite similar except that $\theta(C_3C_1C_3)$ and $\theta(C_4C_2C_4)$ are predicted to be about 1° smaller in $[TCNQF_4]^{\bullet-}$ and $\theta(C_2C_4N)$ is predicted to deviate from linearity by 2.6° in $[TCNQF_4]^{\bullet-}$.

The calculated structure for $[TCNQF_4]^{2-}$ again shows good agreement with the observed structure except for the twist of the $C(CN)_2$ groups with respect to the plane of the benzene ring. The second derivative analysis (see below) shows no negative directions of curvature, so the calculated D_{2h} structure for the dianion is a minimum. However, as discussed below, the frequencies for torsion about the $C_1–C_2$ bond are very small (~20 cm^{-1}) and crystal packing forces could easily lead to the observed distortion. The largest difference between theory and experiment in a bond distance is 0.026 Å for $r(C_3–C_3)$. The C≡N bond distance is larger in $[TCNQF_4]^{2-}$ as compared to $TCNQF_4$ by 0.006 Å but is shorter than the value in $[TCNQF_4]^{\bullet-}$, supporting our previous comment that the UHF formalism leads to an overestimation of this bond distance in $[TCNQF_4]^{\bullet-}$. The calculated bond angles are in excellent agreement with the experimental values in $[TCNQF_4]^{2-}$. Comparison with the calculated structure for $[TCNQ]^{2-}$ shows some differences with $r(C_3–C_3)$ being 0.015 Å longer and $r(C_1–C_2)$ being 0.009 Å longer in $[TCNQF_4]^{2-}$. The angles $\theta(C_3C_1C_3)$ and $\theta(C_4C_2C_4)$ are again smaller in $[TCNQF_4]^{2-}$ than in $[TCNQ]^{2-}$.

The calculated change in structure as negative charge is added follows the results found previously in TCNQ. Although the calculated ring bonds are within 0.011 Å of each other and are approximately aromatic in $[TCNQF_4]^{2-}$, the bond angles do not exhibit the trend of all becoming 120°. In fact, $\theta(C_3C_1C_3)$ deviates more from 120° as charge is added. The exocyclic double bond in $TCNQF_4$ has become almost a single bond in $[TCNQF_4]^{2-}$ as would be expected based on resonance structure A. Resonance structure B also plays a role since $r(C_2–C_4)$ is predicted to decrease

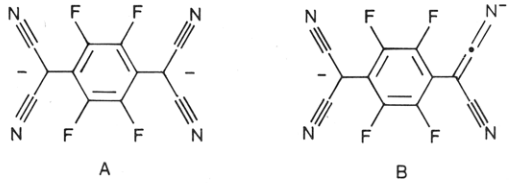

by 0.043 Å. This is consistent with our previous observations in $[C(CN)_3]^-$[25] and TCNQ.[7] Just as found in TCNQ, there is only a slight increase in r(C≡N) going from $TCNQF_4$ to $[TCNQF_4]^{2-}$. An increase in r(C–F) is also predicted as negative charge is added

(25) Dixon, D. A.; Calabrese, J. C.; Miller, J. S. *J. Am. Chem. Soc.* **1986**, *108*, 2582.

TABLE VII: Charge Distributions for $[TCNQF_4]^n$ (n = 0, 1−, 2−) and Spin Distribution for n = 1−

Mulliken Charges, e

atom	n = 0	n = 1−	n = 2−
C_1	0.03	−0.05	−0.02
C_2	0.03	−0.03	−0.17
C_3	0.13	0.08	0.07
C_4	0.08	0.06	0.05
N	−0.15	−0.21	−0.36
F	−0.10	−0.14	−0.16

Spin Populations (e) in $[TCNQF_4]^{\bullet-}$

atom	total	p_z	$p_x + p_y$	2s	spin density
C_1	−0.27	−0.17	−0.06	−0.043	−0.12
C_2	0.74	0.46	0.17	0.112	0.30
C_3	0.04	0.02	0.01	0.007	0.02
C_4	−1.00	−0.40	−0.46	−0.135	−0.36
N	0.98	0.48	0.45	0.046	0.15
F	0.00	0.00	0.00	0.000	0.00

consistent with delocalization of some of the negative charge to the fluorines.

Charges. Mulliken charges are given in Table VII. For neutral $TCNQF_4$, both the N and F are negative and the carbons are positive. The most positive carbons are these bonded to N and F. All of the atoms become more negative as negative charge is added; however, the carbons bonded to N and F still remain positive. Carbons C_1, C_3, and C_4 also gain 0.03–0.05 e of negative charge from n = 0 to n = 2−. The fluorine gains 0.06 e of negative charge. The largest accumulations of negative charge are on C_2 and N which gain 0.20 e and 0.21 e, respectively, consistent with the importance of structures A and B. The fluorines cannot effectively show anionic hyperconjugation[26] because this would lead to strained valence bond structures. The atomic charges have been calculated for $TCNQF_4$[27] and $[TCNQF_4]^{\bullet-}$[21] in the INDO approximation using the geometries derived from the crystal structure. For $TCNQF_4$, the INDO charges are qualitatively similar except that the C–F bond is too polar and C_2 is somewhat too positive as compared to the ab initio results. Similar results are found in $[TCNQF_4]^{\bullet-}$ with both the C≡N and C–F bonds being too polar.

Spins. The spin populations determined from the UHF wave functions for $[TCNQF_4]^{\bullet-}$ are also given in Table VII. The spin populations are defined as the difference between the Mulliken populations for the α- and β-spin electrons (there is one more electron with α spin). Positive spin implies an excess population of α-spin electrons whereas negative spin implies an excess population of β-spin electrons. Excess α spin is found on C_2 and N which have the most negative charge. The C_4 atoms are the most positive and have the most excess β-spin population. The atom C_1 also has a significant excess β-spin population consistent with its charge being more positive than the charge on C_2, which has a large excess α-spin population. There is very little excess spin associated with the C–F bonds. The excess spin on C_1 and C_2 is mostly in the out-of-plane p_z orbital whereas the excess spin on C_4 and N (the C≡N bond) is approximately evenly divided between in-plane and out-of-plane components.

The ESR spectrum is governed by the interactions of the electron spins in the s orbitals with the nuclear spins since the s orbitals are the only ones with a nonvanishing component at the nucleus. On the basis of the 2s orbital populations, we assign the largest ^{13}C hyperfine splitting to be at C_4 and the next largest at C_2. The coupling constants would be of opposite sign and the one at C_4 is negative. The smallest ^{13}C coupling constant would be at C_1 and would be negative. The 2s orbital population on N is of the same magnitude as that at C_1 but the coupling constant is of opposite sign. There is no substantial interaction predicted for C_3 or F.

(26) Dixon, D. A.; Fukunaga, T.; Smart, B. E. *J. Am. Chem. Soc.* **1986**, *108*, 4027.
(27) Kistenmacher, T. J.; Wiygul, F. M.; Emge, T. J. In *Intermolecular Forces*; Pullman, B., Ed.; Reidel: New York, 1981; pp 499–512.

TABLE VIII: Harmonic Frequencies (cm^{-1}) and Infrared Intensities (km/mol) for $TCNQF_4$ and $[TCNQF_4]^{2-}$

$TCNQF_4$				$[TCNQF_4]^{2-}$		
calcd	scale	I	obsd[a]	calcd	scale	I
			a_g			
2716	2227	0	2227	2652	2175	0
1990	1632	0	1665	1882	1543	0
1869	1458[b]	0	1456	1706	1450[d]	0
1475	1328	0	1273	1443	1299	0
994	895	0	878	1017	915	0
696	626	0	620	745	670	0
520	468	0	484	562	506	0
369	332	0	343	376	338	0
292	263	0	298	292	263	0
154	139	0	155[c]	156	140	0
			b_{1g}			
2711	2223	0	2219	2587	2121	0
1687	1518	0	1498	1867	1531	0
1383	1245	0	1230[c]	1393	1254	0
1313	1182	0	1193	1333	1200	0
837	753	0	740[c]	847	762	0
533	480	0	484[c]	569	512	0
453	408	0	423[c]	492	443	0
268	241	0		266	239	0
163	147	0	167[c]	149	134	0
			b_{2g}			
871	784	0		832	749	0
740	666	0		632	569	0
473	426	0	423[c]	463	417	0
238	214	0	222[c]	230	207	0
91	82	0	82[c]	113	102	0
			b_{3g}			
537	483	0	484[c]	563	507	0
431	388	0	378[c]	481	433	0
72	65	0	60[c]	22	20	0
			a_u			
707	636	0		696	626	0
499	449	0		562	506	0
110	99	0		140	126	0
58	52	0		21	19	0
			b_{1u}			
827	744	1		739	665	16
677	609	7	635	623	561	126
288	259	5	257[c]	278	250	1
169	152	19	165[c]	183	165	4
29	26	2		52	47	11
			b_{2u}			
2711	2223	73	2214	2587	2121	460
1953	1601	51	1598	1758	1494	78
1613	1451	23	1394	1352	1217	152
1361	1225	5	1191	1192	1073	135
1108	997	28	976	1128	1015	5
550	495	1	464[c]	583	525	2
336	302	1	330	328	295	0.4
282	254	2	257	279	251	1
110	99	4	94[c]	100	90	3
			b_{3u}			
2718	2229	61	2228	2643	2167	512
1920	1574	89	1551	1732	1472	630
1617	1325	150	1347	1598	1438	737
1259	1133	7	1138	1300	1170	218
886	797	24	806	872	785	17
696	626	2	618	744	670	8
547	492	7	464[c]	543	489	28
326	293	7		339	305	2
175	158	9		178	160	22

[a] Reference 28. [b] Scale factor = 0.78. [c] Assignments based on the calculations. [d] Scale factor is 0.85. Assigned to keep the relative ordering of frequencies correct.

Vibrational Analysis of $TCNQF_4$ and $[TCNQF_4]^{2-}$. The force fields for TCNQ and $[TCNQF_4]^{2-}$ were calculated analytically. The resulting harmonic frequencies are given in Table VIII to-

gether with the infrared intensities. The intensities are only meant to provide qualitative information in the spirit of the strong (s), medium (m), and weak (w) classifications employed experimentally. The calculated frequencies are too high as compared to experiment due to basis set effects, due to neglect of correlation corrections, and because the observed frequencies include anharmonicity effects. We can account for these effects by simply scaling the frequencies. For the C≡N stretches, a scaling factor of 0.82 has been shown to be appropriate. Scale factors of 0.82 are appropriate for the C=C stretches except that the a_g band calculated for $TCNQF_4$ at 1869 cm^{-1} seems to require a smaller scale factor of 0.78. The remaining frequencies have less of a multiple bond stretching component, and a scale factor of 0.90 is appropriate. There are no negative directions of curvature, and thus the structures have the calculated D_{2h} symmetry as noted above.

The agreement between the assigned experimental values[28] and the calculated values for $TCNQF_4$ is quite good considering the size of the basis set. We assign the observed Raman transition at 155 cm^{-1} as an a_{1g} fundamental. There are three observed Raman transitions between 1150 and 1250 cm^{-1}. We prefer assigning the third b_{1g} transition as 1230 cm^{-1} and assign the fourth b_{1g} transition at 1195 cm^{-1}. The observed transition at 740 cm^{-1} should be assigned as a b_{1g} in-plane mode rather than a b_{2g} mode. The observed band at 484 cm^{-1} probably contains both a b_{1g} and b_{3g} transition besides the a_{1g} band. We also assign observed Raman transitions at 423 and 167 cm^{-1} as having b_{1g} symmetry although the transition at 423 cm^{-1} could be of b_{2g} symmetry. We find no evidence for b_{2g} transitions at 740 and 609 cm^{-1} as suggested in the experimental assignments. Observed Raman transitions at 222 and 82 cm^{-1} can be assigned to b_{2g} symmetry whereas transitions at 378 and 60 cm^{-1} can be assigned to b_{3g} symmetry.

The observed infrared transition at 635 cm^{-1} is assigned to b_{1u} symmetry as suggested in the experimental analysis. The infrared transition at 257 cm^{-1} assigned as a b_{2u} mode is essentially coincident with a b_{1u} mode. The transition at 165 cm^{-1} is assigned as a b_{1u} mode. The very low frequency calculated at 26 cm^{-1} was not observed. We assign the observed transition at 464 cm^{-1} as a b_{2u} mode as well as the transition at 94 cm^{-1} although this latter mode does show an inappropriate polarization. The observed IR transition at 464 cm^{-1} could also have a b_{3u} component. Although the IR transition at 165 cm^{-1} that we assigned to b_{1u} symmetry is also consistent with a b_{3u} mode, the polarization is not correct. These results show that our theoretical calculations are useful in assigning the observed experimental transitions.

Only five IR bands in $TCNQF_4$ are predicted to be reasonably intense. The b_{3u} transition at 1347 cm^{-1} is predicted to be the most intense and is indeed a strong band in the spectrum. Both the b_{2u} and b_{3u} CN stretches, 2214 and 2228 cm^{-1}, respectively, are predicted to be reasonably intense as is the asymmetric C=C stretch at 1551 cm^{-1}. The b_{2u} transition at 1953 cm^{-1} is also predicted to be reasonably intense.

Only the two CN transitions for $[TCNQF_4]^{2-}$ can be assigned from our experimental results. The transition at 2167 cm^{-1} is assigned to b_{3u} symmetry and the transition at 2133 cm^{-1} to b_{2u} symmetry. Both are predicted to be quite intense with the lower frequency having a lower intensity just as is observed experimentally. The splitting of the cyano frequencies is only 6 cm^{-1} for TCNQ but is 54 cm^{-1} in $[TCNQF_4]^{2-}$ just as found in comparing TCNQ and $[TCNQ]^{2-}$. The lower frequency of the C≡N stretches in $[TCNQF_4]^{2-}$ as compared to $TCNQF_4$ is consistent with the contribution from resonance structure B.

The frequencies of the C=C stretches decrease in $[TCNQF_4]^{2-}$ as expected due to the change in bonding as the benzene ring is formed. The second b_{1g} frequency calculated at 1867 cm^{-1} is predicted to increase in the dianion as compared to the neutral. Most of the remaining frequencies show only small changes. The lowest energy b_{3g} and a_u torsions are predicted to be only 20 cm^{-1}. In the crystal the molecule distorts along the b_{3g} mode, giving the two $C(CN)_2$ groups in a plane 33.3° twisted from the plane of the benzene ring. The low energy of this torsional mode is consistent with this distortion being due to crystal packing forces.

As noted previously for TCNQ, addition of two negative charges is predicted to significantly increase the infrared intensities. Since the infrared intensity is proportional to $\partial\mu/\partial x_i$ (μ = dipole moment, x_i = normal mode), an increased charge separation between atoms as found in $[TCNQF_4]^{2-}$ can lead to enhanced infrared intensities. As expected, the four highest frequency b_{3u} modes are predicted to be very intense. The b_{2u} CN stretch should be very intense whereas the next two highest b_{2u} modes are of reasonable intensity as is the b_{1u} mode predicted at 623 cm^{-1} (unscaled). When infrared and Raman results become available for $[TCNQF_4]^{2-}$ salts with simpler counterions, these calculations should aid in interpreting the spectra.

Acknowledgment. We appreciate the generous gift of $TCNQF_4$ presented by Dr. R. C. Wheland (Du Pont CR&DD) and synthetic assistance supplied by C. Vazquez and D. Wipf (Du Pont CR&DD).

Registry No. $[Fe(C_5Me_5)_2]_2[TCNQF_4]$, 118458-09-6; $[Co(C_5Me_5)_2]_2[TCNQF_4]$, 118458-10-9; $[Fe(C_5Me_5)_2]_2[TCNQF_4]_2$, 118458-11-0; $[Co(C_5Me_5)_2]_2[TCNQF_4]_2$, 118458-12-1; $[Cr(C_5Me_5)_2]_2[TCNQF_4]_2$, 118458-13-2; $Fe(C_5Me_5)_2$, 12126-50-0; $TCNQF_4$, 29261-33-4; $[Co(C_5Me_5)_2]^{+}[PF_6]^{-}$, 79973-42-5; $Co(C_5Me_5)_2$, 74507-62-3; $Cr(C_5Me_5)_2$, 74507-61-2.

Supplementary Material Available: Interatomic cation bond distances and angles, intermolecular and intramolecular distances, deviations from least-squares planes (7 pages); calculated and observed structure factors for $[Fe(C_5Me_5)_2]_2[TCNQF_4]$ (10 pages). Ordering information is given on any current masthead page.

(28) Meneghetti, M.; Pecile, C. *J. Chem. Phys.* **1986**, *84*, 4149.